Symplectic Particle-In-Cell Method for 1-Dimensional Vlasov-Poisson Plasma System

Jinsu Kim
Department of Mechanical and Aerospace Engineering
Princeton University
jk9075@prineton.edu
https://github.com/ZINZINBIN/APC523Project

May 17, 2025

Abstract

In this project, we integrate the symplectic integration with the Particle-In-Cell method, a mesh-coupling method for kinetic simulation, to simulate a one-dimensional Vlasov-Poisson plasma system. The symplectic integration allows the conservation of the system's Hamiltonian, while the Particle-In-Cell method efficiently computes the dynamics of the plasma. We verify the code by simulating two-stream instability and bump-on-tail instability.

1 Introduction

A plasma is a fourth state of matter that consists of ionized particles such as ions, electrons, and neutrals. It can be interpreted as an electrically conducting fluid [1] where a myriad of charged particles of this system interact with each other and generate self-consistent electromagnetic fields that affect the dynamics of the particles [2]. Among the several approaches to understanding complex dynamics, the plasma kinetic approach is the most fundamental one based on a statistical kinetic model called the Vlasov equation, combined with Maxwell's equations. This is known as the Vlasov-Maxwell equation [3], which can describe the accurate physics of the system [3] and kinetic effects that the general approaches cannot explain. Since this system has a Poisson-bracket structure, it can be described as a Hamiltonian system, indicating that solving the Vlasov-Maxwell equation automatically guarantees that the Hamiltonian of the system is conserved when the plasma is collisionless [4, 5].

Despite this benefit, this approach requires a high computational cost since it is complex to solve and the number of particles is too large to be covered. To reduce the computational cost, the Particle-In-Cell (PIC) method [6], a particle-mesh coupling approach, was suggested. This is based on a Lagrangian frame to track the particles in phase space, while the physical quantities, including densities and fields, are approximated on each mesh instead of being computed for each particle. This enables low computational cost by avoiding the calculation in high-dimensional coordinates for solving the Poisson equation [7]. However, the dissipation of the Hamiltonian can happen during the PIC simulation, even though the system has a Hamiltonian structure. This is due to the time integration, where the general explicit time integration method cannot preserve the Hamiltonian structure well for a long timescale simulation. Thus, symplectic integration for the particles' dynamics is required for PIC simulation.

This project implements the symplectic integration with the PIC method to simulate the kinetics of the plasma while preserving the Hamiltonian of the system. We cover a one-dimensional periodic system with an electrostatic plasma, where the effect of the induced magnetic field is ignored. This allows us to cover the one-dimensional Vlasov-Poisson equation, a simplified equation of the Vlasov-Maxwell equation. For small-scale simulations, we consider the electron motions only while the ions are assumed to be fixed. Our numerical experiments are a two-stream instability [8] in which two electron beams in different directions

are injected, and a bump-on-tail instability [9] where the high-energy electron perturbation is added in the thermalized electron plasma. The external perturbation applied to the system induces the plasma-wave interaction and results in a shape of a separatrix in a phase-velocity space of the system [10] and reaches a new equilibrium of the velocity distribution where the quasi-linear diffusion can be observed. We will cover the plasma dynamics with the Vlasov-Maxwell equation and then explain how to implement the code and numerical results in the following sections.

2 Plasma Dynamics

Plasma can be treated as an electric fluid that contains particle interactions (collision) and field-particle interactions. The motion of the plasma induces a change in the distribution of charged particles, which generates electromagnetic fields and affects the motion again. The self-consistent behaviors of the fields and particles can be described by integrating the fluid and Maxwell's equations, which allows us to understand the dynamics of a continuous medium interacting with fields. First, we can describe the electric field E and magnetic field B by following Maxwell's equations below.

$$\nabla \cdot E = 4\pi \sum_s q_s n_s = 4\pi\rho \tag{1}$$

$$\nabla \times E = -\frac{1}{c}\frac{\partial B}{\partial t} \tag{2}$$

$$\nabla \cdot B = 0 \tag{3}$$

$$\nabla \times B = \frac{4\pi}{c}\sum_s q_s n_s v_s + \frac{1}{c}\frac{\partial E}{\partial t} = \frac{4\pi}{c}J + \frac{1}{c}\frac{\partial E}{\partial t} \tag{4}$$

where n_s, q_s, and c are the number density, the electric charge of the species s, and the speed of light, respectively. Here, the electric density ρ and current density J are given as $\rho = \sum_s n_s q_s$ and $J = \sum_s q_s n_s v_s$. Since these equations require information about the distribution of particles, such as charge density and current density, the following fluid equations are to be solved.

$$\frac{\partial n_s}{\partial t} + \nabla \cdot n_s v_s = 0 \tag{5}$$

$$m_s n_s \frac{dv_s}{dt} = q_s n_s (E + v_s \times B) - \nabla P_s \tag{6}$$

$$\frac{d}{dt}\left(\frac{P_s}{n_s^\gamma}\right) = 0 \tag{7}$$

From Equation 5 to 7, m_s, v_s, and P_s are the mass, velocity, and pressure of the species s, respectively. This model assumes that P_s follows the adiabatic process. Combining Equation 1 to 7, we can understand the dynamics of the plasma fluid interacting with its self-consistent electromagnetic field. However, this approach has limitations since the fluid approach assumes the collisionality of the plasma and ignores the kinetic effect, including the interaction between two different types of particles. Therefore, the kinetic approach has been introduced and combined with plasma dynamics as an alternative and more accurate way.

3 Vlasov-Maxwell Equation

Plasma kinetic approach focuses on the particle distribution function, determined by a governing equation called the Vlasov-Maxwell equation. The Vlasov-Maxwell equation is a differential equation for the time-evolving distribution function for a collisionless plasma that has a long-range interaction with an order of the Debye length based on the Boltzmann equation for a kinetic approach [3]. Equation 8 is a form of the Vlasov-Maxwell equation where f_s is a particle distribution function of species s. If the correlation between

different particles is considered, the RHS of the equation is not zero. However, we will cover the collisionless case where the correlation can be ignored.

$$\frac{d}{dt}f_s(x,v,t) = \frac{\partial}{\partial t}f_s(x,v,t) + v\cdot\nabla_x f_s(x,v,t) + \frac{q_s}{m_s}(E + v\times B)\cdot\nabla_v f_s(x,v,t) = 0 \tag{8}$$

If the collision term is ignored, the Vlasov-Maxwell equation satisfies the conservation of the moments in phase space. The total number, momentum, and Hamiltonian are zeroth, first, and second order moments, which can be derived by integrating the distribution function with v^n over velocity, where n indicates n-th moment. For the zeroth and first order moment, the conservation equations are equivalent to Equation 5 and 6. In the case of a second-order moment, the Hamiltonian can be computed as Equation 9.

$$H[f] = \sum_s \int \frac{1}{2}m_s v^2 f_s(x,v,t)dxdv + \int \frac{1}{8\pi}(E^2 + B^2)dx \tag{9}$$

Now, the Hamiltonian contains the distribution function since not only the kinetic energy term but also the fields are given from the distribution function from 1 to 4 combined with 10, 11, and 12.

$$n(x,t)_s = \int f_s(x,v,t)dv \tag{10}$$

$$\rho_s(x,t) = q_s\int f_s(x,v,t)dv \tag{11}$$

$$J(x,t) = \sum_s \int q_s v f_s(x,v,t)dv \tag{12}$$

4 Poisson-Bracket and Hamiltonian structure of Vlasov-Maxwell equation

The Vlasov-Maxwell equation has a Poisson-Bracket structure, which follows the defined Poisson bracket notation for two functionals [11]. If F and G are given as two functionals of the distribution function f, then the definition of the bracket is described as equation 13.

$$\{F,G\}(f) = \int f\{\frac{\delta F}{\delta f},\frac{\delta G}{\delta f}\}dxdv + \int fB\cdot(\frac{\partial}{\partial v}\frac{\delta F}{\delta f}\times\frac{\partial}{\partial v}\frac{\delta G}{\delta f})dxdv \tag{13}$$

where the operator $\{\cdot,\cdot\}$ is the canonical Poisson bracket for two functions for x and v as equation 14.

$$\{f,g\} = \frac{\partial f}{\partial x}\cdot\frac{\partial g}{\partial v} - \frac{\partial f}{\partial v}\cdot\frac{\partial g}{\partial x} \tag{14}$$

$\frac{\delta F}{\delta f}$ is the variational derivative for f. Since the magnetic field satisfies $\nabla\cdot B = 0$, the following system is now described as equation 15 when we set $G = H[f]$.

$$\frac{dF}{dt} = \{F,H\}_f = \int f\{\frac{\delta F}{\delta f},\frac{\delta H}{\delta f}\}dxdv \tag{15}$$

If we additionally set $F[f] = \int f(\tilde{x},\tilde{v},t)\delta(x-\tilde{x})\delta(v-\tilde{v})d\tilde{x}d\tilde{v}$ and $H[f]$ as $H[f] = \int[\frac{1}{2m}(p-\frac{q}{c}A)^2 + q\phi]fdxdp$, then the Poisson bracket leads to the following equation as 16.

$$\frac{\partial f}{\partial t} = -\{f,h\} - B\cdot(\frac{\partial f}{\partial v}\times\frac{\partial h}{\partial v}) \tag{16}$$

where $h(x,v) = \frac{\delta H}{\delta f} = \frac{1}{2}mv^2 + q\phi$. Equation 16 is equivalent to Hamilton's equation, meaning that this structure can be converted to the Hamiltonian structure by the following procedures. If the system is canonical

and described in phase space, we can derive a multi-variable chain rule to get the time derivative of the distribution function in phase space.

$$\frac{df}{dt} = \frac{\partial f}{\partial x}\frac{dx}{dt} + \frac{\partial f}{\partial p}\frac{dp}{dt} + \frac{\partial f}{\partial t} \tag{17}$$

where p is momentum in phase space. If the dynamics in this system follow Hamilton's equations, then the following equations are satisfied.

$$\frac{dx}{dt} = \frac{\partial H}{\partial p} = \{x, H\} \tag{18}$$

$$\frac{dp}{dt} = -\frac{\partial H}{\partial x} = \{p, H\} \tag{19}$$

Therefore, the time derivative of the distribution function can lead to equation 20.

$$\frac{df}{dt} = \{f, H\} + \frac{\partial f}{\partial t} \tag{20}$$

This is equivalent to equation 16 when the LHS equals zero. Note that Equation 16 is derived from the Vlasov-Maxwell equation, indicating that the system has the Poisson-Bracket structure. From equation 20, a collisionless plasma system that follows the Poisson-Bracket structure can have the Hamiltonian structure. This implies two things. First, the Vlasov-Maxwell equation describes the dynamics of the Hamiltonian system. Second, the collisionless plasma conserves the Hamiltonian structure, so the energy is also preserved. We can compute the Hamiltonian of the collisionless plasma system as Equation 9 and describe the system as a linear ODE formula as Equation 21.

$$\frac{dz}{dt} = J\nabla_z H \tag{21}$$

where $z = [x_1, x_2, ...x_n, p_1, p_2, ...p_n]^T$ and $J = \begin{pmatrix} O_n & I_n \\ -I_n & O_n \end{pmatrix}$ while $J^T J = JJ^T = I_{2n}$ and $JJ = -I_{2n}$. This symplectic structure is equivalent to $\frac{dz}{dt} = \{z, H\}$.

5 Particle-In-Cell Method for Plasma Kinetic Simulation

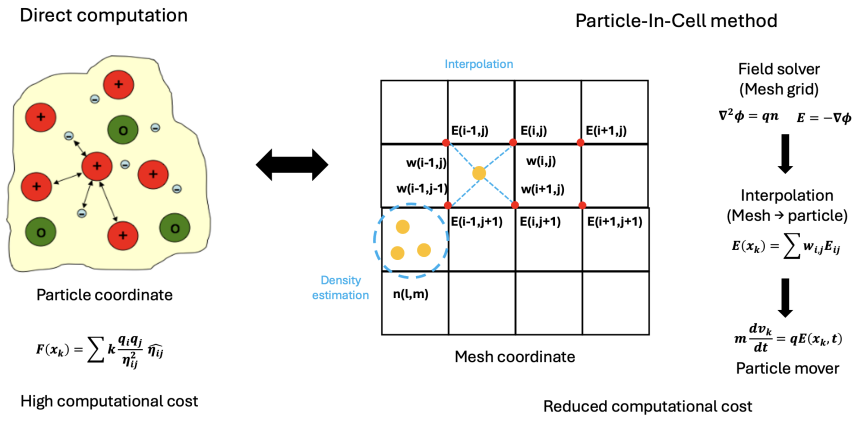

Figure 1: Basic concept and scheme of the Particle-In-Cell method

Particle-In-Cell method [6] is a particle-mesh coupling method for solving equations of motion in kinetic systems. The main concept of this method is to separate the particle coordinate and mesh coordinate

for electromagnetic fields. While a Lagrangian frame to track the particles in phase space is applied on the particle coordinate, the physical quantities like densities and fields are approximated on a coarse mesh coordinate, which allows the reduction of the computational cost for solving Maxwell's equations [7]. Figure 1 compares direct computation and the PIC method. Note that there is an interpolation process that maps the field computed on the mesh coordinate to the particle coordinate. For each iteration, the field solver calculates E and B on a mesh grid, and the interpolated fields are applied to update the state of the particles.

Although PIC is easy to implement and enables a low computational cost for field calculation, the dissipation of the Hamiltonian is a problem since a general explicit time integration method cannot preserve the Hamiltonian structure for a long timescale simulation. Thus, we utilize the symplectic integration known as a 2nd-order Verlet method (Leapfrog). The details for developing the symplectic PIC code are described in Figure 2.

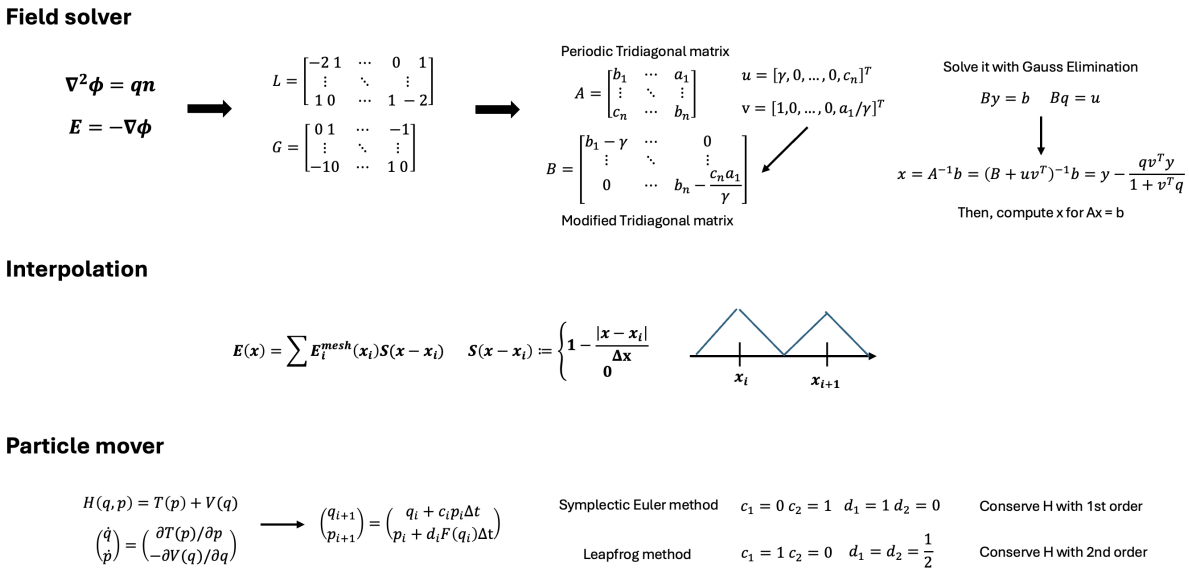

Figure 2: The detailed computational processes of the Particle-In-Cell method

As mentioned in the previous section, our system is periodic and electrostatic. Thus, our field solver calculates E only by solving the Poisson equation on the mesh coordinate. Then, we can get the approximate electric field at the particle coordinate by the interpolation process. The particle mover updates the state of the particles while the Hamiltonian structure is preserved. The following explanations describe the details of the implementation for each step.

Field solver We apply the second-order Finite Difference Method in the one-dimensional case to discretize the Laplacian and gradient operators. The periodic condition is applied to the boundary of the matrix. To solve this linear equation, we utilize the Thomas algorithm with the Sherman-Morrison formula [12, 13], since the Laplacian is not a tridiagonal matrix. Instead of solving $Ax = b$, we can make tridiagonal matrix $B = A - uv^T$, where $u = [\gamma, ..., c_n]^T$ and $v = [1, ..., a_1/\gamma]^T$. Here, a_1 and c_n are $L_{1,N}$ and $L_{N,1}$, respectively. γ is a parameter to be chosen. Then, we can solve $q = B^{-1}u$ and $y = B^{-1}b$ to get the solution $Ax = b$ from the Sherman-Morrison formula, which is the real solution given as $x = y - \frac{qv^T y}{1+v^T q}$.

Interpolation We apply the Triangular Shape Cloud (TSC), a 2nd-order interpolation method [14], to approximate the projected electric field on the particle coordinate.

Particle mover The symplectic integration methods are employed in this process. Our system is a canonical Hamiltonian system, where the coordinate includes position and momentum for each particle and satisfy Equation 21. Thus, Hamilton's equations are satisfied for each particle. We select the Leapfrog method for structure-preserving time integration during the particle move step.

6 Numerical Simulations

Our numerical experiments contain two cases: Two-stream instability [8] and bump-on-tail instability [10]. Figure 3 describes initial conditions for two cases, where Equation 22 and 23 indicate the initial velocity distribution for the two-stream instability and bump-on-tail instability, respectively. Two-stream instability is observed when two electron beams with opposite directions are injected into a plasma system where the background ions are fixed. The injected beam has a Gaussian distribution with mean velocity $v_0 = \pm v_b$. This induces plasma-wave interaction via the electric field and leads to plasma-wave excitation. Bump-on-tail instability generally occurs when the high-energy electron beam is injected into the thermalized electrons. The high-energy electron beam injection results in a bump on the tail of the velocity distribution of the thermalized electrons. The bump on its tail is dissipated by the quasi-linear diffusion in the velocity space, reaching a new equilibrium.

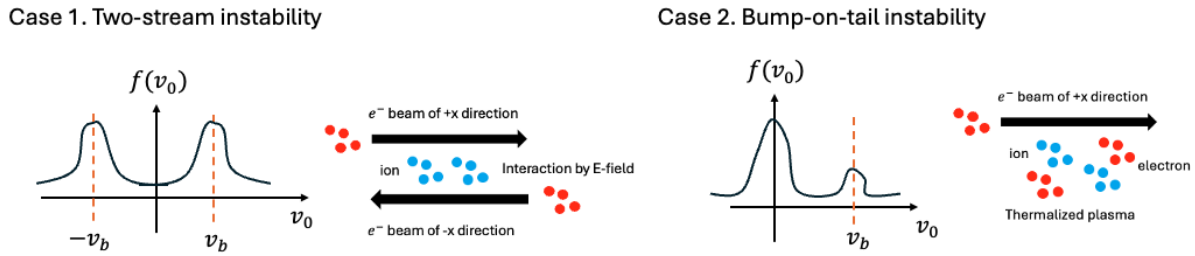

Figure 3: Visual description for two-stream instability and bump-on-tail instability

$$f(v_0) = \frac{1}{2\sqrt{2\pi}} e^{-\frac{1}{2}(v_0 - v_b)^2} + \frac{1}{2\sqrt{2\pi}} e^{-\frac{1}{2}(v_0 + v_b)^2} \tag{22}$$

$$f(v_0) = \frac{1}{(1+a)\sqrt{2\pi}} e^{-\frac{1}{2}v_0^2} + \frac{a}{(1+a)\sqrt{2\pi}} e^{-\frac{1}{2\sigma^2}(v_0 - v_b)^2} \tag{23}$$

For both cases, we add the sinusoidal wave perturbation in the initial velocity with respect to the position where $v(x, 0) = v_0(1 + A \sin 2\pi n_{mode} \frac{x}{L})$. PIC simulation requires the spatial resolution condition $\Delta x < 3.4\lambda_{Debye}$ and temporal resolution condition $\Delta t < 2\omega_{pe}^{-1}$ to be satisfied for numerical stability. Therefore, we set $N = 40000$, $N_{mesh} = 1000$, $L = 50$, $\Delta t = 0.01$. The other parameters are $v_b = 3.0$, $a = 0.2$, $\sigma = 0.5$, $A = 0.02$, and $n_{mode} = 5$ during simulation.

6.1 Two-stream instability

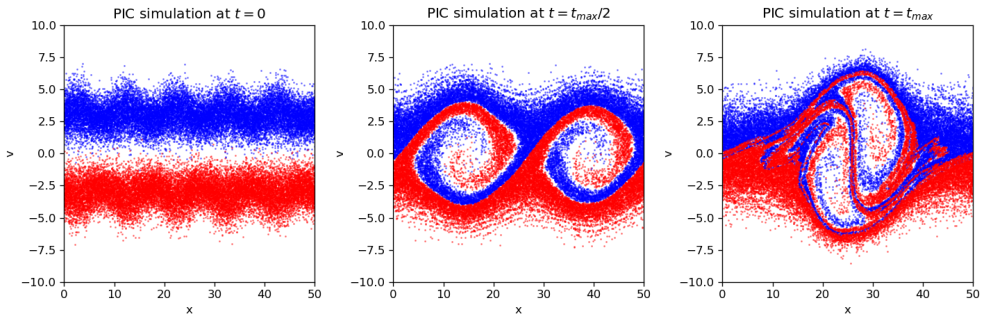

Figure 4: The evolution of the plasma state in a phase space during the two-stream instability simulation

The numerical simulation for the two-stream instability with parameters and setup given in the previous section is described in Figure 4. We can see the separatrix induced by the evolution of the sinusoidal velocity perturbation due to plasma-wave interaction in a phase space. Here, the blue particles represent

the high-energy electron beam injected in the $+x$ direction, while the red particles are in the $-x$ direction. Interestingly, the mode number n_{mode} of the initial perturbation is 5, but the plasma-wave interaction causes the formation of the two different separatrices in a phase space. These are eventually combined to form a complex structure.

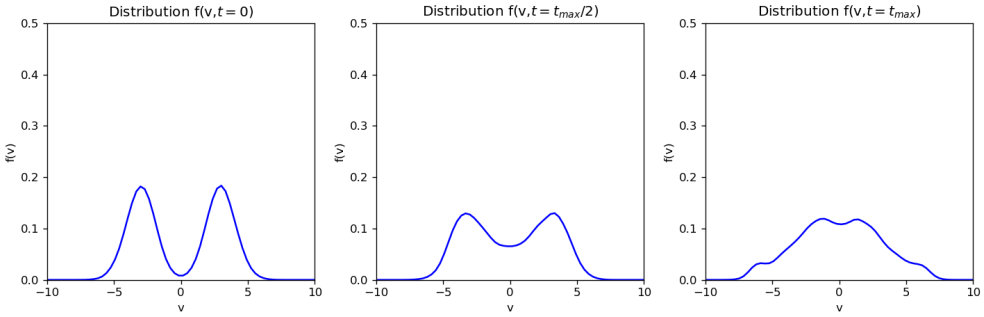

Figure 5: The evolution of the velocity distribution during the two-stream instability simulation

Figure 5 shows the time evolution of the velocity distribution for two-stream instability, which corresponds to the time evolution of the plasma state in Figure 4. We can see that the initial Gaussian distributions with two different mean values are combined to reach a new equilibrium at the end of the simulation. This is also due to the plasma-wave interaction in a plasma system, while the two different beams interact through an induced electric field.

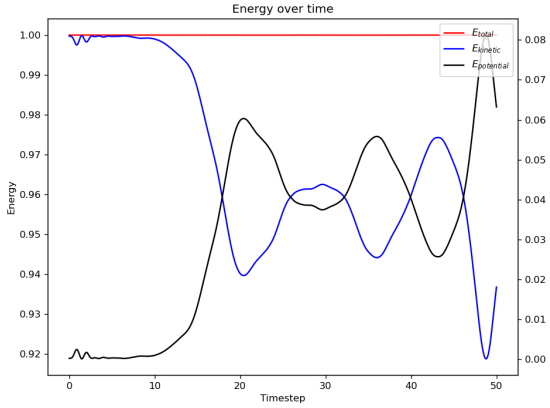

Figure 6: The energy of the system over time during the two-stream instability simulation (red: total energy, blue: plasma kinetic energy, black: electric potential energy)

Figure 6 represents the system's energy over time in the two-stream instability simulation. The figure indicates that the symplectic integration conserves the Hamiltonian over time for a long-time simulation. Here, the drastic decrease in the kinetic energy corresponding to the peak of the electric potential energy near $t = 20s$ and $t = 50s$ is observed. Note that this corresponds to the time when the formation of the separatrix happens in Figure 4. Again, our symplectic PIC code shows the conservation of the Hamiltonian based on the Leapfrog method during the two-stream instability simulation.

6.2 Bump-on-tail instability

Similarly, we simulated the bump-on-tail instability as described in Figure 7. In this case, the red particles are high-energy injected electrons, whereas the blue particles are thermalized. Due to plasma-wave interaction, the formation of the separatrix in a phase space is observed in the middle of the time. At the same time, Figure 8 shows that there is a plateau regime at the tail of the velocity distribution, which results from the quasi-linear diffusion in the velocity space. This is an example of Landau-damping [15], where the electrons' energy is transferred to other regimes by wave propagation through an electric field.

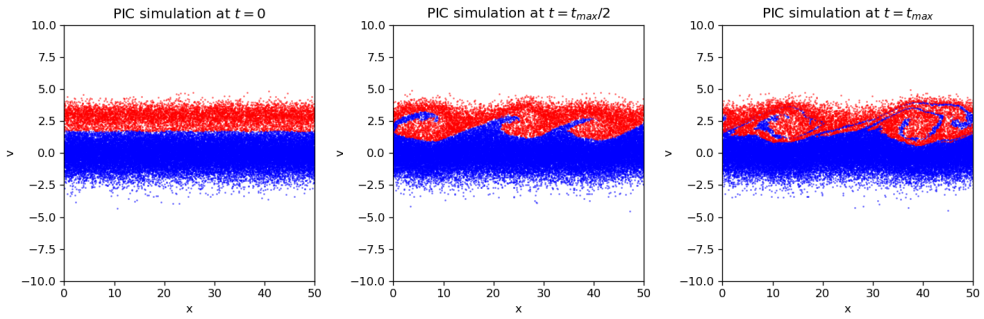

Figure 7: The evolution of the plasma state in a phase space during the bump-on-tail instability simulation

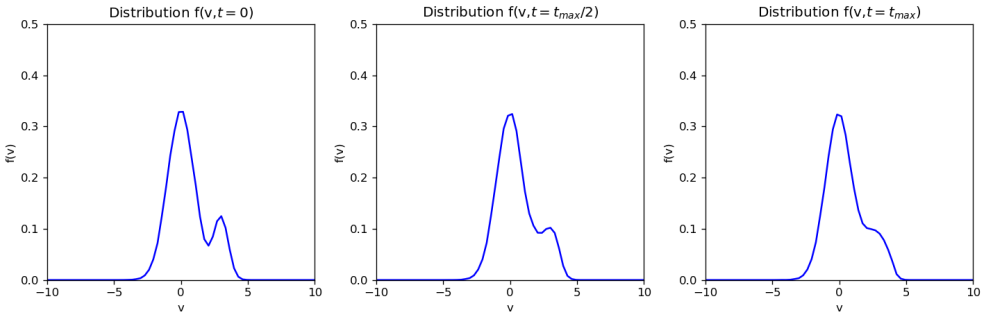

Figure 8: The evolution of the velocity distribution during the bump-on-tail instability simulation

Lastly, Figure 9 represents the system's energy over time in the bump-on-tail simulation. As mentioned in the two-stream instability case, the symplectic integration conserves the Hamiltonian over time for a long-time simulation.

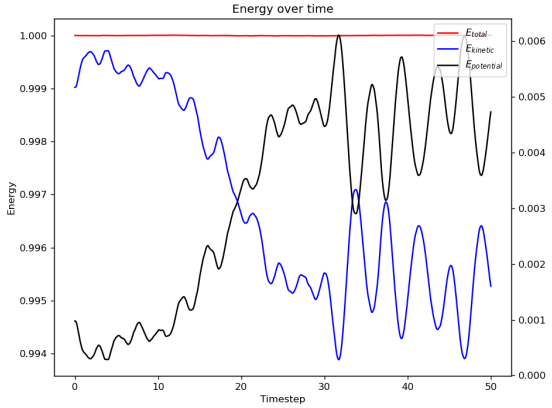

Figure 9: The energy of the system over time during the bump-on-tail instability simulation (red: total energy, blue: plasma kinetic energy, black: electric potential energy)

7 Discussion

Here, we analyze the numerical stability, accuracy, and time complexity of our algorithm with two-stream instability simulation, since the bump-on-tail instability simulation cannot be executed with low spatial and temporal resolution cases. Our reference simulation setting is the same as mentioned in the previous

section. For stability analysis, we first compare the grid resolution while changing N_{mesh}, and then change the time difference dt to check numerical stability with respect to the temporal resolution condition. For accuracy analysis, we change N_{mesh} to observe the energy conservation error and simulation error compared to the reference case. Finally, we will see the computational time required for computing the field and particle mover with different N and N_{mesh}.

7.1 Stability and energy conservation

In PIC, the spatial resolution condition $\Delta x = L/N_{mesh} < 3.4\lambda_{Debye}$ and the temporal resolution condition $\Delta t < 2w_{pe}^{-1}$ are required for numerical stability with the leapfrog method. These conditions guarantee the conservation of the Hamiltonian structure and energy conservation. From the parameters used in this simulation, $\lambda_{Debye} = v_{th}/w_{pe}$ and $w_{pe} = \sqrt{N/L}$ while $e = \epsilon_0 = m_e = 1$ for convenience. To analyze the numerical stability, we plotted the energy over time to check the conservation, instead of using the linear stability analysis, since the interpolation of the electric field cannot be linearized. Figure 10 and Figure 11 represent the system's energy over time with different grid mesh sizes and time differences, respectively. Note that the cases where $N_{mesh} = 200$ and $N_{mesh} = 400$ violate the spatial resolution condition $L/N_{mesh} < 3.4\lambda_{Debye}$, while the cases where $dt = 0.10$ and $dt = 0.50$ violate the temporal resolution condition. These cases show a violation of energy preservation during simulation, meaning that the numerical stability is violated and induces energy dissipation in the system.

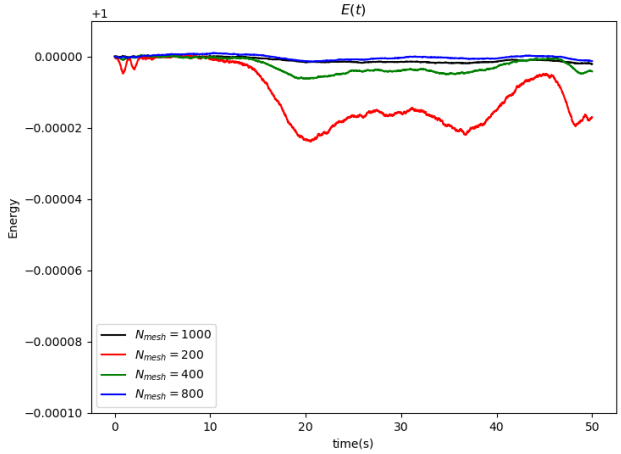

Figure 10: The total energy over time during the two-stream instability simulation with different N_{mesh}

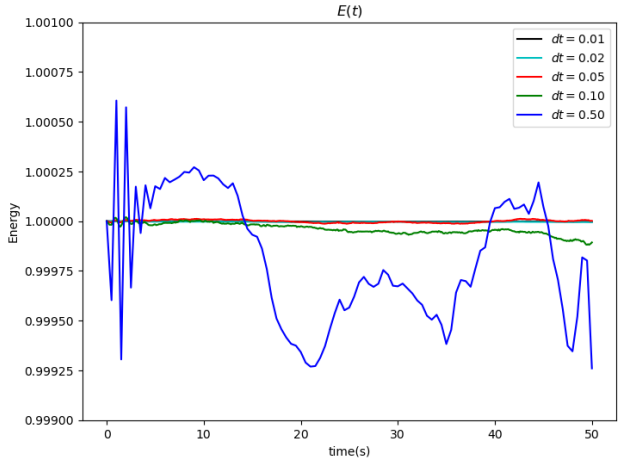

Figure 11: The total energy over time during the two-stream instability simulation with different dt

7.2 Numerical accuracy

PIC code approximates the electric field of the system by computing the quantity on a coarse grid, reducing computational cost during simulation. This means that the spatial resolution related to N_{mesh} determines the accuracy of the simulation. Furthermore, dt determines not only the numerical stability, but also the numerical error for time integration. Thus, we analyze the L_2 error of the state vector compared to the reference case with different N_{mesh} and dt, which are described by Figure 12 and Figure 13. We can see that the numerical errors are accumulated during the simulation for all cases, but the lower resolution cases have higher errors. Figure 14 and 15 represent the total average L_2 error of the state vector with different mesh sizes and time differences, respectively. Again, the temporal and spatial resolutions can also decide the numerical error.

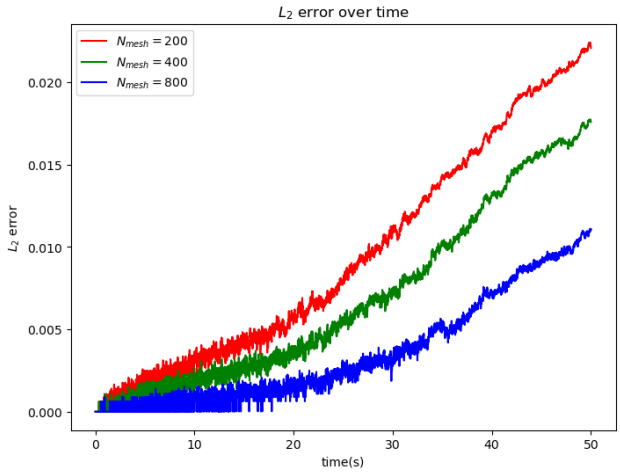

Figure 12: Average L2 error of the state vector during the two-stream instability simulation with different N_{mesh}

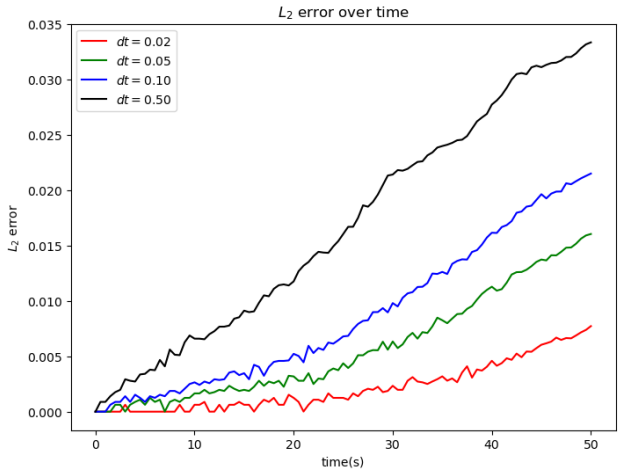

Figure 13: Average L2 error of the state vector during the two-stream instability simulation with different dt

8 Conclusion

In this work, we developed the symplectic plasma kinetic code for a one-dimensional periodic electrostatic plasma system. Based on PIC method, we can describe the plasma kinetic effect, including the quasi-linear diffusion and instabilities induced by the perturbation. Applying symplectic integrators allows

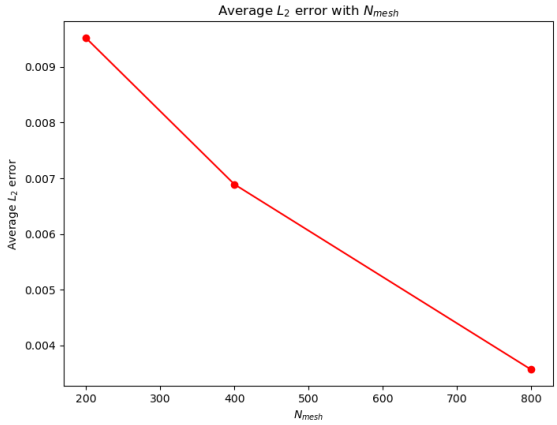

Figure 14: Total average L2 error of the state vector over time with different N_{mesh}

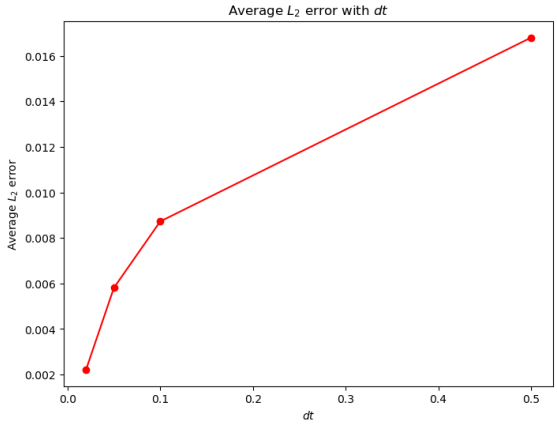

Figure 15: Total average L2 error of the state vector over time with different dt

the PIC code to conserve the Hamiltonian of the system during the long-time simulation, which are verified in this project. Furthermore, TSC interpolation and the Thomas algorithm with the Sherman-Morrison formula can efficiently calculate the electric field on a coarse mesh coordinate and approximate it on a particle coordinate with high accuracy. In the future, we can further develop the multi-dimensional PIC code where the electromagnetic plasma is considered. High-order interpolation and symplectic integration methods would be considered for higher simulation accuracy.

References

[1] Jeffrey P Freidberg. *ideal MHD*. Cambridge University Press, 2014.

[2] Robert J Goldston. *Introduction to plasma physics*. CRC Press, 2020.

[3] Donald Gary Swanson. *Plasma kinetic theory*. Crc Press, 2008.

[4] Jerrold E Marsden and Alan Weinstein. The hamiltonian structure of the maxwell-vlasov equations. *Physica D: nonlinear phenomena*, 4(3):394–406, 1982.

[5] Joseph K Miller, Andrea R Nahmod, Nataša Pavlović, Matthew Rosenzweig, and Gigliola Staffilani. A rigorous derivation of the hamiltonian structure for the vlasov equation. In *Forum of Mathematics, Sigma*, volume 11, page e77, 2023.

[6] David Tskhakaya, Konstantin Matyash, Ralf Schneider, and Francesco Taccogna. The particle-in-cell method. *Contributions to Plasma Physics*, 47(8-9):563–594, 2007.

[7] Anjiao Gu, Yang He, and Yajuan Sun. Hamiltonian particle-in-cell methods for vlasov–poisson equations. *Journal of Computational Physics*, 467:111472, 2022.

[8] TM O'neil and JH Malmberg. Transition of the dispersion roots from beam-type to landau-type solutions. *Physics of Fluids*, 11(8):1754–1760, 1968.

[9] Magdi Shoucri and Lutz Angermann. Numerical simulation of the bump-on-tail instability. *Numerical Simulations, Applications, Examples, and Theory*, pages 3–38, 2011.

[10] Luiz Fernando Ziebell, Rudi Gaelzer, and Peter H Yoon. Nonlinear development of weak beam–plasma instability. *Physics of Plasmas*, 8(9):3982–3995, 2001.

[11] Herbert Goldstein, Charles Poole, John Safko, and Stephen R Addison. Classical mechanics, 2002.

[12] Milan Batista and Abdel Rahman A Ibrahim Karawia. The use of the sherman–morrison–woodbury formula to solve cyclic block tri-diagonal and cyclic block penta-diagonal linear systems of equations. *Applied Mathematics and Computation*, 210(2):558–563, 2009.

[13] J Shermen and WJ Morrison. Adjustment of an inverse matrix corresponding to changes in the elements of a given column or a given row of the original matrix. *Annual Mathmatical Statistics*, 20:621–625, 1949.

[14] Giovanni Lapenta. Particle in cell methods. In *With Application to Simulations in Space. Weather*. Citeseer, 2016.

[15] L Landau. On the vibrations of the electronic plasma. *Zhurnal eksperimentalnoi i teoreticheskoi fiziki*, 16(7):574–586, 1946.